Received: 26 April 2020 | Revised: 1 July 2020 | Accepted: 29 July 2020

DOI: 10.1111/ina.12727

WILEY

ORIGINAL ARTICLE

Quantitative profiling of built environment bacterial and fungal communities reveals dynamic material dependent growth patterns and microbial interactions

Ying Xu[1] | Ruby Tandon[2] | Chrislyn Ancheta[2] | Pablo Arroyo[2] | Jack A. Gilbert[3] | Brent Stephens[4] | Scott T. Kelley[1,2]

[1]Graduate Program in Bioinformatics and Medical Informatics, San Diego State University, San Diego, CA, USA

[2]Department of Biology, San Diego State University, San Diego, CA, USA

[3]Department of Pediatrics and Scripps Institution of Oceanography, University of California San Diego, La Jolla, CA, USA

[4]Department of Civil, Architectural, and Environmental Engineering, Illinois Institute of Technology, Chicago, IL, USA

Correspondence
Scott T. Kelley, Graduate Program in Bioinformatics and Medical Informatics, San Diego State University, 5500 Campanile Drive, San Diego, CA 92182, USA.
Email: skelley@sdsu.edu

Funding information
Alfred P. Sloan Foundation

Abstract

Indoor microbial communities vary in composition and diversity depending on material type, moisture levels, and occupancy. In this study, we integrated bacterial cell counting, fungal biomass estimation, and fluorescence-assisted cell sorting (FACS) with amplicon sequencing of bacterial (16S rRNA) and fungal (ITS) communities to investigate the influence of wetting on medium density fiberboard (MDF) and gypsum wallboard. Surface samples were collected longitudinally from wetted materials maintained at high relative humidity (~95%). Bacterial and fungal growth patterns were strongly time-dependent and material-specific. Fungal growth phenotypes differed between materials: spores dominated MDF surfaces while fungi transitioned from spores to hyphae on gypsum. FACS confirmed that most of the bacterial cells were intact (viable) on both materials over the course of the study. Integrated cell count and biomass data (quantitative profiling) revealed that small changes in relative abundance often resulted from large changes in absolute abundance, while negative correlations in relative abundances were explained by rapid growth of only one group of bacteria or fungi. Comparisons of bacterial-bacterial and fungal-bacterial networks suggested a top-down control of fungi on bacterial growth, possibly via antibiotic production. In conclusion, quantitative profiling provides novel insights into microbial growth dynamics on building materials with potential implications for human health.

KEYWORDS

16S rRNA, bacterial diversity, built environment, culture-independent methods, FACS analysis, fungal diversity, indoor microbial ecology, ITS-1, live-dead cell sorting, microscopy counting, next-generation sequencing, quantitative abundance

1 | INTRODUCTION

The built environment (BE) is the sum total of all habitable artificial structures and includes, but is not limited to, apartments, houses, office buildings, shopping malls, restaurants, and enclosed modes of transportation. It has been estimated that humans in industrialized nations spend up to 90% of their time inside the BE.[1,2] This shift toward indoor living has also created unique habitats for microorganisms, especially bacteria and fungi, with novel selection pressures that likely shape microbial evolution.[3] During the past two decades,

there has been a substantial effort from researchers around the world to apply culture-independent molecular methods (eg, amplicon and metagenomic sequencing) and computational methods to characterize the microbial ecology and distribution dynamics of the BE.[4-8]

Despite the overall diversity of indoor microbial systems being increasingly well described, the molecular characterization has occurred predominantly on dry surfaces.[9] Culture-independent microbiology studies in wet BE environments have primarily focused on sinks, toilets, water pipes, and other surfaces specifically designed for high levels of moisture,[10] but the effects of moisture on microbial dynamics on materials such as wood materials and drywall have received much less attention.[11,12] Dry surface studies have proven highly useful for understanding the source and movement of microbes in the BE,[13] and the effects of BE design on indoor microbial diversity.[14] However, surfaces are also an "ecological desert" with a largely inactive microbial community.[9] Culture-based studies have long showed the importance of water for stimulating microbial growth, both fungal and bacterial.[15-17] Fungal growth and material decay typically occur at RH conditions above 75%, depending on building material type.[18] Approximately 50% of homes in the United States have experienced dampness or the occurrence of visible mold[19] due to plumbing leaks, flooding, groundwater entry or insufficient ventilation.[20] Depending upon the extent of water damage and environmental factors, Indoor Air Quality can decrease significantly in damp buildings due to increased levels of volatile compounds, microbial particulate matter and mycotoxins, sometimes resulting in serious health problems.[21-25]

The vast majority of studies investigating the impact of moisture on microbial growth in the BE have used traditional culturing techniques. However, recent studies have applied multiple -omics techniques to investigate bacterial, fungal, and even metabolic growth dynamics at a community-level scale.[10] In particular, Lax et al applied a multi-omics approach using amplicon sequencing of 16S rRNA and ITS rRNA gene markers, metabolomics, and fluorescent microscopy to investigate bacterial-fungal interactions over time on different building materials exposed to liquid water and high humidity conditions.[26] The results of this study revealed the dramatic effects of wetting on bacterial/fungal diversity, including high microbial growth rates, low alpha-diversity, material-specific communities, and evidence of metabolic and competitive interactions within and between the bacterial and fungal communities.

In addition to -omics technologies, culture-independent biomass analysis can provide insight into microbial community

Practical Implications

- Our combinatorial approach linking bacterial cell counting, fungal biomass, and live/dead staining directly to amplicon sequencing of bacterial and fungal communities provided new insights into the effects of wetting and material type on growth patterns in built environments. Specifically, we showed a strong material and time-dependent effect on bacterial and fungal growth and diversity.
- Fungal/bacterial interactions were very different between material types, including among fungi and bacteria known for antibiotic production and resistance, respectively.
- Our results provide a road map for studying how different materials encourage the growth of microbes over time and how they also may contribute to the development of antibiotic resistance.

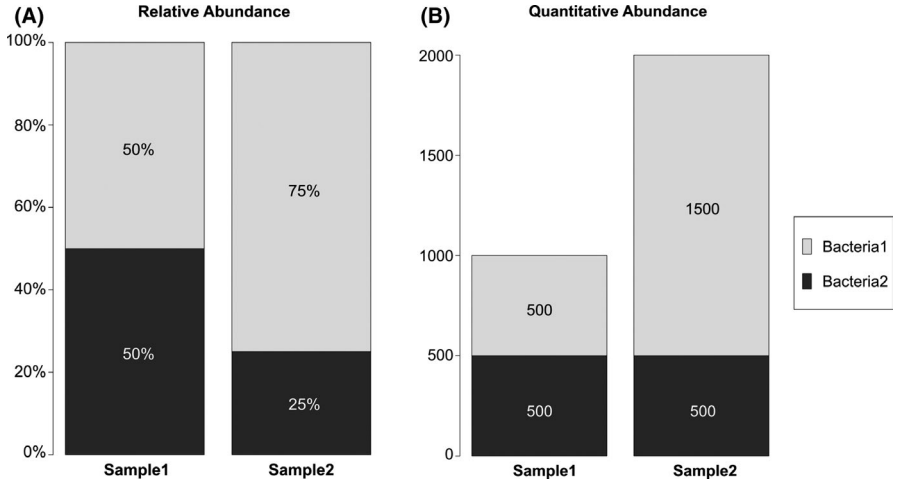

FIGURE 1 Comparison between relative (A) and quantitative abundance (B). Quantitative abundance is calculated with biomass 1000 for sample1 and 2000 for sample2. In relative profiling, the abundance of bacteria2 from sample1 to sample2 appears to decrease, while the abundance of bacteria1 appears to increase (ie, they are negatively correlated). However, after adjusting for cell counts via quantitative profiling, we observed that the abundance of bacteria2 did not change, while the abundance of bacteria1 tripled, meaning that the negative correlation was an artifact of the compositional nature of the sequence data. Vandeputte *et al* (2017) used a similar principle to show that a purported trade-off between *Bacteriodes* and *Prevotella* was an artifact of relative microbiome analysis[70]

dynamics. Culture-independent counting techniques, such as DNA/RNA staining of bacterial cells and viral-like particles (VLPs), have often been used in other environments and have proven highly useful for characterizing ecosystem biomass and ecological interactions.[27,28] Methods such as fluorescence-assisted cell sorting (FACS) and qPCR, both of which can be used to quantify bacterial abundances, can aid in the interpretation of ecological interactions.[29,30] However, these methods have rarely been applied to the BE; as such, our best understanding of BE microbial ecology and dynamics is based on relative abundance counts from amplicon or metagenomic sequencing approaches. Results from the few studies applying quantitative methods show their potential for illuminating differential growth patterns on various materials types under different environmental conditions and for quantifying total indoor VLP or bacterial particle abundances in the BE.[26,31,32] Recently, Vandeputte et al showed that these data can also be directly incorporated into sequence-based microbial profiling. Not only did they find microbial load, per se, to be a significant indicator of disease state, they also showed that "quantitative profiling" (combining biomass data with sequencing data) corrected for artifacts imposed by the compositional nature of sequence data analysis (Figure 1).

Here, we built upon the Lax et al results by performing a new study that combined three culture-independent microscopy methods with deep sequencing analysis of bacterial and fungal communities to perform quantitative profiling of building material microbial communities impacted by wetting and high humidity. We hypothesized that the combination of biomass analysis and quantitative profiling would significantly change the interpretation of microbial community growth on different materials compared with sequence-only based relative abundance profiling, and reveal strong time-dependent patterns of microbial growth and composition. Using a replicated repeated measures design (Figure 2), we followed the growth and evolution of naturally formed communities on two common building material types: medium density fiberboard (MDF) and gypsum wallboard (referred to as "gypsum"). Amplicon sequencing of the 16S and ITS rRNA genes was used to characterize bacterial and fungal microbial diversity. To quantitate microbial growth and biomass, we applied bacterial- and viral-like particle counting, light microscopy for fungal-fungal biomass estimation, and FACS to determine patterns of bacterial, viral, and fungal growth on MDF and gypsum over time. We also quantitatively profiled the microbial communities by combining bacterial cell counts and fungal microscopy results with the 16S and ITS rRNA amplicon sequencing data. Our results show that quantitative data by itself, and in combination with compositional taxonomic data, provides deeper insight into the growth and evolution of BE microbial communities and can significantly alter the interpretation of microbial interactions.

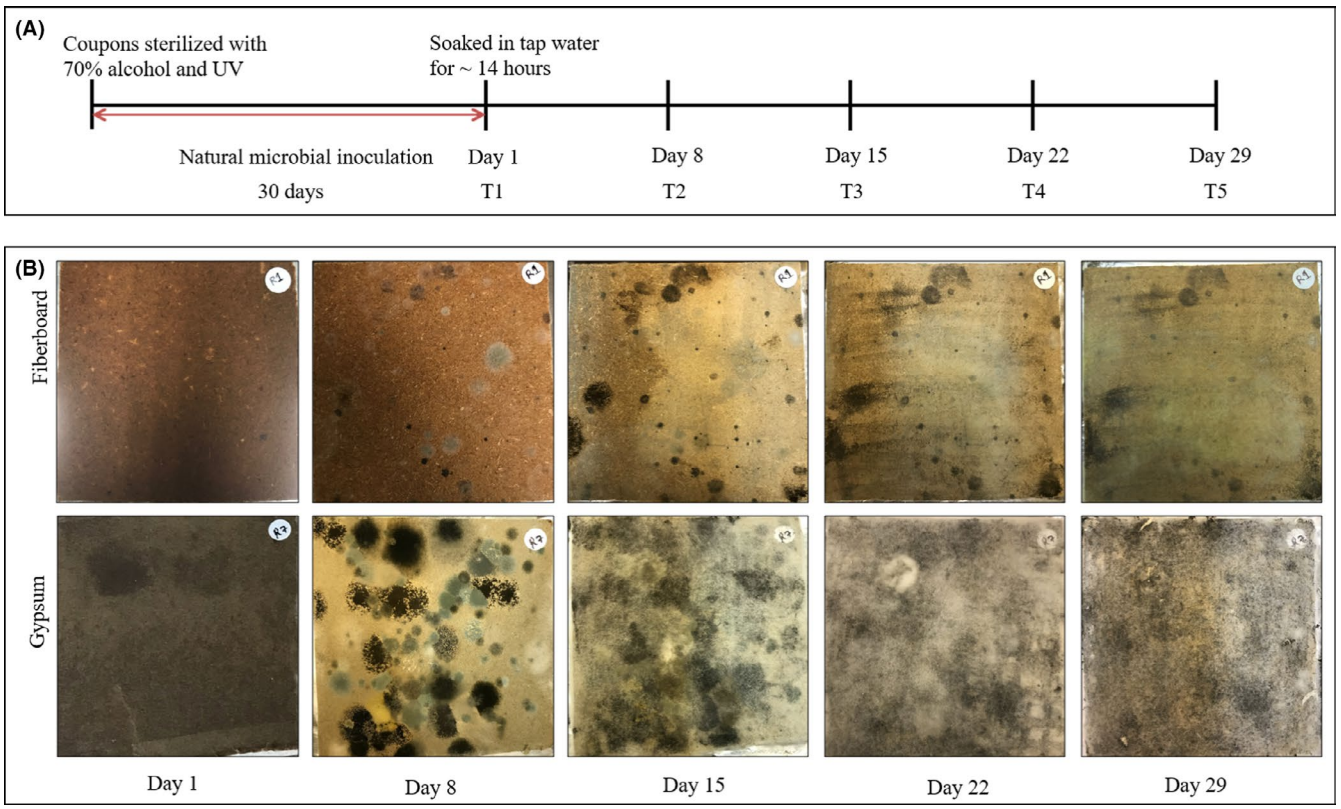

FIGURE 2 (A) Study timeline. After sterilization, coupons for medium density fiberboard (MDF) and gypsum were naturally inoculated for 30 d and soaked in tap water. Coupons were swabbed on days 1, 8, 15, 22, and 29. (B) Pictures of coupons of both the material types taken at different points

2 | METHODS

2.1 | Sample collection

Two building material types were used for this study: gypsum wallboard and medium density fiberboard (MDF). These materials were cut into 10 cm × 10 cm identical sized coupons, and the coupon surfaces were sterilized using ultraviolet light and 70% ethanol solution. Three duplicate coupons of each material were naturally inoculated with indoor microbial flora. Both sets of coupons were placed open to the environment on a bench inside the sitting area of our laboratory at San Diego State University and left undisturbed for 30 days. The top surface was marked, and the same side was swabbed at different time points in the study. To encourage fungal growth on each material, all of the material coupons were soaked in tap water for ~14 hours. They were then moved to trays and were incubated at 25°C inside an incubator. Individual coupons were sealed in airtight plastic containers with a supersaturated potassium nitrate (KNO3, Sigma-Aldrich) solution was used to maintain high relative humidity (RH) near ~95% for the duration of the experiment.[33] Temperature and RH in the chamber air were recorded every 10 minutes using an Onset HOBO U12 data logger. A check of the log showed that the RH did not drop below 90% over the course of the experiment. Samples for microbiological analysis, microscopy, 16S rRNA and ITS sequencing were preserved in 0.85% NaCl solution, 4% paraformaldehyde and 1X phosphate buffer saline (PBS). All solutions were prepared with 0.02 μm filtered molecular biology grade Sigma water. Samples were taken at 5 weekly time points: T1, T2, T3, T4, and T5. T1 was collected immediately after soaking the materials in water for ~14 hours. To maintain the constant RH, the containers were opened only briefly to swab the coupons (approximately 5 seconds) before resealing the containers. Thereafter, samples were collected at each time point (every 7 days). BD Screw Cap SWUBE™ Polyester swabs were used for sampling coupon surfaces. A set of three coupons was re-swabbed for each material type at each time point. The entire coupon surface was passed over once with a swab in one direction. The tips were broken off into 1.5 mL microtubes containing 700 μL 0.85% NaCl solution (prepared using 0.02 μm filtered Sigma water) and vortexed for 20 seconds. A total of 200 μL was preserved for microscopy in 4% paraformaldehyde. A total of 250 μL was aliquoted separately and used for live-count counts using flow cytometry and for DNA extractions. The rest of sample was preserved for sorting live-dead cells using FACS. All the samples were stored at −80°C before further analysis.

2.2 | Viral-like particle and bacterial microscopy counts

Epifluorescence microscopy was used to estimate abundance of virus-like particles and bacteria in all the samples. Samples fixed using paraformaldehyde were thawed on ice before staining. A total of 100 μL of PFA-fixed sample was resuspended in 5 mL of 0.02 μm filtered Sigma water (Sigma-Aldrich). The diluted sample was then filtered onto 0.02 μm anodisc filters (Whatman). The filters were stained with 1X SYBR Gold in dark for 10 minutes and washed with filtered water for 5 minutes. SYBR Gold binds to nucleic acids in cells (excitation—300nm, 495 nm; emission—537 nm). The disks were mounted on the glass slides and imaged on an Olympus 60× object magnification oil-immersion microscope connected to QImaging Retiga EXi Fast Cooled Mono 12-bit microscope. Images were analyzed using Image Pro software (Media Cybernetics) to estimate VLP and bacterial abundance, with size cutoffs for VLPs between 0.02 and 0.2 microns and bacteria between 0.2 and 10 microns.

2.3 | Fungal spore counts and measuring hyphae length

The 0.02 μm Anodisc filters used for VLP, and bacterial counts were imaged at 20× and 40× magnification with a Zeiss AxioPlan 2e fluorescent microscope equipped with an AxioCam HrM monochromatic camera. Images were analyzed using open source ImageJ software.[34]

2.4 | Flow cytometry analysis and sorting

Flow cytometric analysis was carried out using LIVE/DEAD BacLight bacterial viability kit (Catalog number: L34856, Thermo Fisher Scientific). The assay consists of two fluorescent dyes with different cell permeability characteristics that can be used to differentiate cells on the basis of their membrane integrity. SYTO 9, a green fluorescent dye, penetrates cells with both intact and damaged membrane and, thus, labels all cells. Propidium iodide (PI), a red fluorescent stain, can only penetrate cells with damaged membranes. Therefore, this two-stain combination differentially labels viable and non-viable cells, which can then be enumerated using flow cytometer. Figure S1 shows the workflow for flow cytometry experiments. Samples were thawed on ice, and 20 μL sample volume was stained using 1.5 μL of 3.34 mmol/L SYTO 9 nucleic acid stain and 1.5 μL of 30 mmol/L propidium iodide. Ten μL of microsphere standard beads (concentration of 1.0 × 108 beads) (6 μm diameter) was added to each reaction to serve as reference standard for sample volume. Total volume of reaction was 1 mL. The rest of volume was made up using a 0.85% NaCl solution. The reaction mixture was incubated for 15 minutes on ice for staining. Analysis was performed with a BD (Beckson-Dickson) FACS Canto using the high-throughput sampler unit. Fifty μL of sample was analyzed on standard mode using the 488 nm excitation laser for PI and SYTO 9 fluorescence. Three technical replicates were analyzed for each sample. Cells stained with PI were captured in PerCP-Cy5-5 channel (670 nm long-pass filter preceded by a 655 nm long-pass mirror), and cells stained with SYTO 9 were captured in FITC channel (530/30 nm band-pass filter preceded by a 502 nm long-pass mirror). To ensure consistency between different experimental days, a preparation of dead *E coli* cells (fixed

with 4% PFA) at different dilutions—1:5, 1:100 and 1:500 were analyzed with every experiment. Flow rate was maintained at 0.5 μL/second. The populations were gated based on the intensity in the FITC (for dead cell population) and PerCP (for live cell population) channel. The numbers of live and dead bacteria were calculated using the following formulas:

$$\text{Number of live bacteria} = (\text{number of events in live region}) / (\text{number of events in bead region}) \times \text{concentration of beads} \times \text{dilution factor}$$

$$\text{Number of dead bacteria} = (\text{number of events in dead region}) / (\text{number of events in bead region}) \times \text{concentration of beads} \times \text{dilution factor}$$

Data were collected using FACSDiva 6.1.1. FCS files were exported and analyzed using FCS Express 6. Live and dead bacterial populations were sorted using BD FACS Aria I. PI and Syto 9 stained cells were excited using 488nm laser. The two fractions were sorted into 15 mL conical tubes containing 5 mL of 1× PBS. Samples were moved to dry ice immediately after sorting and stored at −80°C.

2.5 | DNA extraction and sequencing

For each coupon, 150 μL of sample stored in 0.85% NaCl solution was used for DNA extraction. The sorted fractions of live and dead cells were pelleted at 6000 g for 5 minutes, which was suspended in 150 μL of 1× PBS. DNA extractions were performed using PowerSoil DNA Isolation kit (MoBio Laboratories, Inc) as directed by the manufacturer. Genomic DNA was quantified using a Nanodrop spectrophotometer (Thermo Fisher Scientific). Extracted DNA samples were stored at −80°C.

The DNA obtained from the extractions was used for amplification of both 16S rRNA/ITS region. For each sample, the V4 region of the bacterial 16S rRNA gene was amplified using the primer pairs 515F/806R. For the fungal ITS sequencing, we amplified the highly variable internal transcribed spacer region 1 located between the 5.8S and 18S rRNA genes, using the ITS1f and ITS2 primer pairs.[35] Each of the reverse primers (806R and ITS2) had a unique 12 base pair barcode for sample identification. Both the 16S and ITS amplification reaction used the same reaction mixture and thermocycling conditions. The parameters for PCR were as follows: (1) 94°C for 3 minutes, (2) 94°C for 45 seconds, (3) 50°C for 60 seconds, (4) 72°C for 90 seconds, (5) Steps (2)-(4) were repeated 35 times, (6) 72°C for 10 minutes, and (7) 4°C HOLD. Five μL of PCR product was loaded on 2% agarose gel to check 300 bp amplified product. The rest of the PCR product was stored at −80°C. Two negative controls consisted of Sigma molecular biology grade water extracted by the DNA extraction protocol described above. Sequencing was performed on the Illumina MiSeq platform.

2.6 | 16S rRNA sequencing data processing

Sample barcodes were extracted from sequencing files with forward reads using the QIIME1 extract_barcodes script.[36] Raw sequence reads were then imported into QIIME2 (version 2019.01) in "EMP protocol" multiplexed single-end fastq format with the qiime tools import method.[37] Sequences were later demultiplexed using qiime demux emp-single method. DADA2 software[38] in QIIME2 was used for quality filtering (denoising) and generating output sequence variants (SVs) using the q2-dada2 plugin denoise-single method. Reads with quality score lower than 25 were removed. SVs were taxonomically classified using a pre-trained Naive Bayes classifier based on Greengenes 13_8 99% OTUs from 515F/806R region of sequences.[39] Results were filtered to only include features classified at least at the class taxonomic level. Retained SVs were then used to generate a phylogenetic tree using align-to-tree-mafft-fasttree pipeline from the q2-phylogeny plugin.[40,41]

2.7 | ITS sequencing data processing

Barcode extraction, denoising, and sequence-quality filtering for the ITS data were performed in the same manner as with the 16S rRNA sequencing data. For the taxonomic classification of fungal ITS sequences, a custom BLAST database was built using the QIIME release of UINTE database (UNITE Community (2019): UNITE QIIME release for Fungi. Version 18.11.2018. UNITE Community. https://doi.org/10.15156/BIO/786334). SVs were then blasted against this custom database. SV identifiers were later replaced with UNITE database identifiers according to BLAST results, and reads with the same identifiers were grouped together. A pre-built ghost tree[42] using the same version of UNITE database was generated with a midpoint root using the FastTree program[41] to incorporate phylogenetic information. In addition, the q2-feature-table filter-features method[43] was implemented to match ghost-tree tips with SV sequences.

2.8 | Data analysis

Statistical analyses of bacterial- and viral-like particle counts, fungal spores and hyphal-length estimates, and FACS live/dead ratios were performed in R (version 3.5.2). The following data analysis and visualization methods were used on both the 16S rRNA and ITS datasets. Feature tables, taxonomy tables, and phylogenetic trees were initial generated as QIIME2 artifacts9, and the biomformat package (version 1.10.1)[44] was used to export these datasets into R (version 3.5.2)[45] compatible formats for downstream analysis. Relative (proportional) abundance was generated through dividing each read count by the total number of reads in that sample. Quantitative abundances were then generated using a custom R script (available at https://github.

com/vera-yxu/Thesis-QuantitativeAnalysis) which multiplied epifluorescence microscopy cell counts, or a combination of spores and hyphal-length measurements, per sample to the proportional abundance of each bacterial or fungal taxonomic group, respectively. The Phyloseq package (version 1.26.1)[46] was used for manipulating data and preparing for further analyses including visualizations with ggplot2 (version 3.2.0)[47] was implemented for data visualization. Log_2-fold analysis was performed using the DESeq2 package (version 1.22.2)[48] in R. DESeq2 is a deferential expression analysis that uses normalization factors to adjust for the differences in library depth. Correlation analyses of relative and quantitative abundances, and visualization of correlation matrices, were implemented using the corrplot package (version 0.84).[49] Correlations were performed on the relative abundances or quantitative abundances following Vandeputte et al. Relative and quantitative abundances were calculated separately and summed at the genus level, and they had to be present in at least 10% of the samples to be included in the analyses. Network analysis was performed with the igraph package (version 1.2.1.4).[50] Jupyter notebook scripts, including the datasets, for the Phyloseq, DESeq2, corrplot, and igraph analyses are all available for

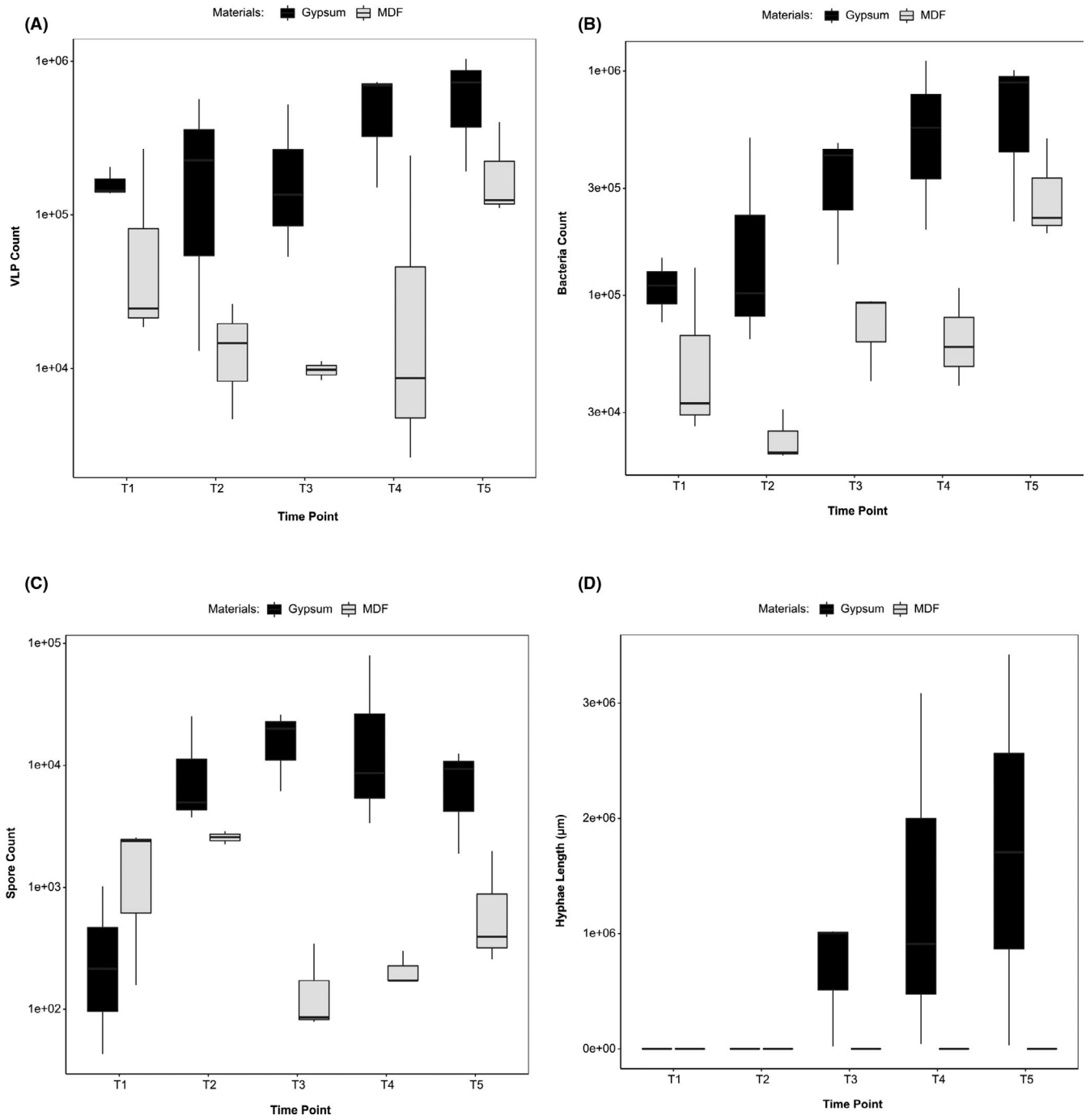

FIGURE 3 Box plots of mean abundances of VLP (A) and bacterial (B) fungal spores (C) and fungal hyphae (D) on gypsum (n = 3) and MDF (n = 3) resampling coupons over a period of 29 d

download at the github link: https://github.com/vera-yxu/Thesis-QuantitativeAnalysis.

To compare beta-diversity, Bray-Curtis[51] and Weighted UniFrac[52] distance matrices were generated and visualized using principal coordinates analysis (PCoA). Feature tables were rarefied to even sampling depths (a rounded number approximately 90% of lowest sampling depth) using q2-diversity core-metrics-phylogenetic method,[53] with distance metric artifacts generated at the same time. The rarefied feature tables were then converted to relative abundance with the q2-feature-table relative-frequency method. The q2-diversity pcoa-biplot method[54] was implemented to generate biplot artifacts. Finally, PCoA plots were visualized using the EMPeror plugin[55,56] in QIIME2 with taxa biplots overlaid.

3 | RESULTS

3.1 | Visible growth on coupons

Coupon images (Figure 2) showed higher visible fungal growth on the paper-covered surface of gypsum compared to MDF. Fungal growth was visible on both types of materials by the first week. Gypsum coupons were completely covered with fungi by day 15 (time point 3). Figure 3 shows that mean VLP and bacteria abundances increased after wetting on both material types. Bacterial and VLP abundances were consistently higher on gypsum compared to MDF. Estimates of fungal biomass were obtained by combining spore counts and hyphal-length measurements. Except for time point 1, box plots revealed a higher spore counts on gypsum coupons than MDF (T1; Figure 3C). Evidence of fungal hyphae growth was detected only on gypsum coupons and only by the third week of the experiment. The mean hyphae length was highly variable (Figure 3D).

Similar to previous studies, both Pearson's and Spearman's coefficients between VLPs and bacterial abundances were > 0.8 (Table 1), indicating a strong linear relationship.[26,31] Positive, albeit weaker, correlations were also detected between bacteria cell counts and fungal spore counts and VLPs and fungal spore counts (Table 1). Type II ANOVAs for VLP, bacterial and fungal counts identified a statistical interaction between material and time with fungal spores counts (Table 2). On MDF coupons, mean spore abundances peaked at T2 before declining substantially by T3 and then increasing slightly, while on gypsum mean spore abundances were greatest at T3 (Figure 3C). On gypsum coupons, hyphae increased at T3 when we observed germination of spores (Figure 4; pers. obs.). Hyphae were not observed on slides made from MDF coupons (Figure 3D).

To further characterize interactions between material and time point, interaction contrasts were performed for counts of VLPs, bacteria, fungal spores, and fungal hyphae length (Table 2; Figure S2). Both microbial and fungal growth were higher on gypsum (Figure S2B, C), indicating that the gypsum wallboard was more supportive of microbial growth after wetting. Comparison of interaction contrasts over time for VLP and bacteria found an initial depression in counts (at T2 and T3), followed by an increase (Figure S2A). Fungal biomass on gypsum increased continuously over the course of the experiment, while growth on MDF was characterized by a sharp increase followed by a decline after week 2 (Figure S2C). Figure S3 shows example images of spores and hyphae from the coupons.

Figure S4 shows comparisons of the number of live and dead cells estimated by FACS analysis over time on the different material types. The increased trend in the number of live and dead cells on gypsum coupons during initial time points corroborated the microscopy count data for both microbes and fungi. The abundances of both live and dead cells differed between materials and among time points, and there was a significant interaction between material type and time with live cells (Table 3).

3.2 | Sequencing data

A total of 3 412 839 16S rRNA sequence reads were generated from a total of 98 amplicon libraries from the same sequencing run. Trimming at position 252 during DADA2 quality filtering[38] in QIIME[37] resulted in a total of 1 565 387 sequence reads belonging to 1317 SV features (n = 96, sequence reads in PCR control2 and extraction control2 samples were 0 after DADA2). The number of SV features was declined to 945 after filtering taxonomy annotation results to only include SVs classified at class level or lower (n = 93, all sequences in MDF2 at TP3 and TP4, MDF3 at TP4 were filtered out).

ITS rRNA sequencing generated a total of 1 406 950 reads from 46 amplicon libraries (MDF3 at TP1 and gypsum2 at TP1 were absent due to low DNA concentration). A total of 1 062 966 reads were kept after trimming at position 244 during DADA2 filtering10, belonging to 297 SV features. One amplicon library sample (gypsum

TABLE 1 Values of Pearson product moment correlation and Spearman's coefficient for abundance counts of VLPs, bacteria and fungi spores

	Pearson product moment correlation		Spearman's coefficient		
	df	*P*-value	Correlation constant	*P*-value	*rho*
VLP:Bacteria	28	$1.072e^{-08}$	0.84	$1.09\ e^{-06}$	0.81
VLP:Fungal_Spores	28	.023	0.41	.019	0.43
Bacteria:Fungal_Spores	28	.004	0.51	.006	0.50

at TP1) was filtered out after denoising. SVs were grouped into 151 features after replacing SV IDs with UNITE database IDs according to BLAST results. Out of 151 SV features, 138 of them that matched to ghost-tree tips were used for generating UniFrac distances an PCoA biplots (the MDF sample at TP0 was filtered out because no reads mapped to the pre-built ghost tree).

After removing the PCR and negative extraction control samples, which had negligible sequence counts, we were left with a total of 27 16S rRNA amplicon libraries. From these sample swab samples, we successfully generated 23 amplicon libraries for 16S rRNA FACS separated live-only samples, and 24 FACS separated dead-only samples (Figure S1). Bacterial and VLP counts were generated for all 27 whole-community samples. After removing the PCR and negative control samples, we were left with 28 ITS amplicon library samples; fungal spore counts and hyphae length data were generated for 23 of these samples.

TABLE 2 ANOVA (Type II) on microscopy counts ~ material and time

Interaction	*df*	Sum Sq	*F*-Value	*P*-value	Significance
VLP counts					
Material	1	33.0	20.9	1.86 e^{-04}	***
Time	4	5.3	2.7	.058	.
Material:Time	4	3.6	0.8	.516	
Bacterial counts					
Material	1	14.3	29.5	2.57 e^{-05}	***
Time	4	14.1	7.3	8.79 e^{-04}	***
Material:Time	4	2.2	1.1	.367	
Fungal spore counts					
Material	1	34.8	28.2	3.35 e^{-05}	***
Time	4	16.0	3.2	.033	*
Material:Time	4	38.0	7.7	6.26 e^{-04}	***

Note: Significance codes: 0 "***" 0.001 "**" 0.01 "*" 0.05 "." 0.1 " " 1

Figure 5 shows a sample by sample comparison of relative and quantitative bacterial taxonomic abundances on MDF and gypsum. Gypsum samples had higher bacteria quantitative abundance than MDF samples and showed a pattern of steady bacterial growth over time. Growth was discontinuous on MDF samples with the greatest abundances on all the coupons at the final time point. Figure 6 shows a sample by sample comparison of relative and quantitative (combination of spore counts and hyphae lengths) fungal taxonomic abundances on MDF and gypsum. Fungal growth on gypsum was also more pronounced than on MDF, with approximately three times greater biomass abundance, and there were completely different growth patterns on the two materials (Figure 6). For MDF, fungal growth spiked at TP2 and then dropped significantly by TP3. In contrast, there continued to be a steady amount of biomass after TP2 on gypsum surfaces.

Beta-diversity PCoA biplots using weighted UniFrac and Bray-Curtis distances, respectively, determined that weighted UniFrac explained more of the variation in the first 3 principal coordinates for both the bacterial (total percent variation weighted UniFrac = 55.7%, Figure 7A; Bray-Curtis = 26.1%, Figure 7B) and fungal (weighted UniFrac = 83.6%, Figure 7C; Bray-Curtis = 62.5%, Figure 7D) datasets. The PCoA plots identified clear visual separation of both bacterial and fungal communities, which was confirmed by PERMANOVA tests (P = .002 for 16S community with weighted UniFrac and P = .001 for all other 3; Figure 7), but R^2 values were higher with the fungal communities (Figure 7C,D) than with the bacterial communities (Figure 7A,B). The results of

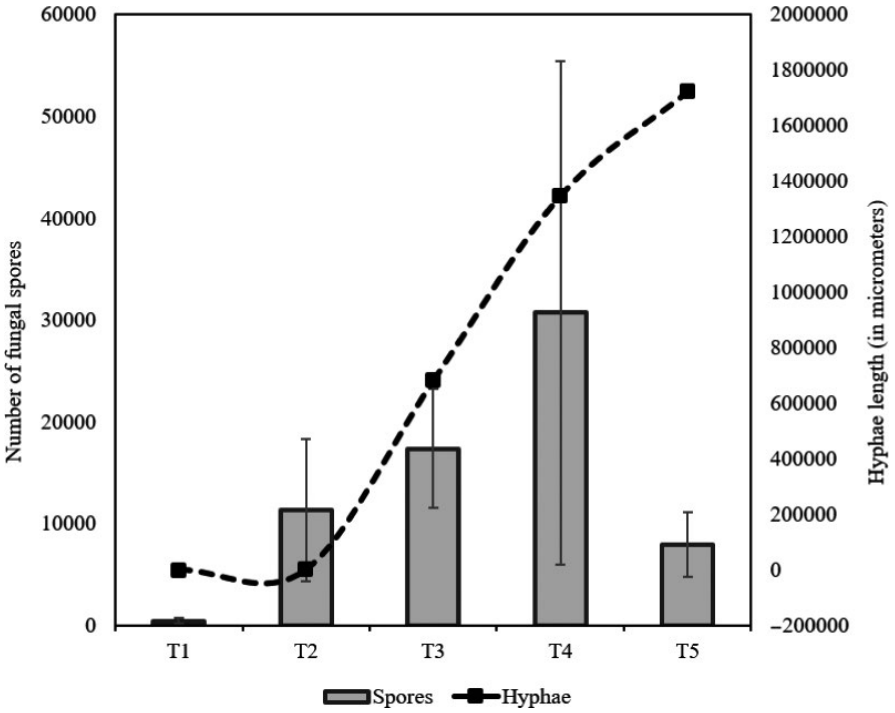

FIGURE 4 Relationship between number of spores and hyphae length over time on gypsum resampling coupons

TABLE 3 ANOVA (Type II) on flow cytometry cell counts ~ material and time

Interaction	*df*	Sum Sq	*F*-Value	*P*-value	Significance
Live cell counts					
Material	1	11.5	70.7	$5.33\ e^{-08}$	***
Time	4	32.8	50.3	$3.69\ e^{-10}$	***
Material:Time	4	5.9	9.1	$2.41\ e^{-04}$	***
Residuals	20	3.3			
Dead cell counts					
Material	1	20.3	37.1	$5.91\ e^{-06}$	***
Time	4	44.5	20.3	$8.06\ e^{-07}$	***
Material:Time	4	2.3	1.0	.41	
Residuals	20	11.0			

Note: Significance codes: 0 "***" 0.001 "**" 0.01 "*" 0.05"." 0.1 " " 1

the $\log_2$-fold analysis with relative abundance data are shown in Figure 8. The bacterial *Staphylococcus*, *Acinetobacter*, and *Thermus* were relatively higher on MDF compared with gypsum, while *Pseudomonas*, *Bacillus*, and *Sphingobium* were higher on gypsum compared with MDF (Figure 8A). For the fungal data, members of the genera *Trichodema*, *Naganishia*, and *Cladosporium* were higher on MDF, while *Didymella*, *Acremonium*, and *Lecanicillium* were relative higher on gypsum (Figure 8B). We also found differential material-specific abundances of a number of *Aspergillus* and *Penicillium* SVs (Figure 8B).

Pearson correlations were used to detect potential interactions between bacteria, between fungi, and between bacteria and fungi. For these analyses, we grouped taxa at the genus level for both bacteria and fungi, and only kept taxa prevalent in at least 10% of the samples. Figure 9 shows the results of correlation tests using both relative and quantitative abundance counts for bacteria-bacteria (Figure 9A) and fungi-fungi (Figure 9B) interactions on MDF coupons. In general, the addition of quantitative data increased the number of significant interactions detected for both bacteria and fungi. The number of significant interactions (Pearson's: $P < .05$; $rho > 0.3$) increased from 10 to 12 with the bacteria and from 15 to 28 with the fungi. In comparison with the MDF coupons, we determined many more statistical correlations with both bacteria and fungi on the gypsum, particularly the bacteria for which we detected almost 5 times more correlations (Figure 9). On gypsum surfaces, the number of correlations did not change dramatically after incorporating quantitative data. However, in the fungi-fungi correlation matrix, five negative correlations were detected with the quantitative data that were not detected with relative abundance data.

Correlation analysis of the combined bacteria and fungi datasets revealed the number of total correlations (bacteria–fungi) was much greater on gypsum than MDF (Figure 10). Additionally, *Penicillium* was negatively correlated with a set of bacteria but were positively correlated with *Bacillus* (Figure 10B). Finally, correlations were visualized as a series of co-occurrence networks. Comparisons of networks generated using relative and quantitative profiling for bacteria-bacteria, fungi-fungi, and bacteria-fungi on MDF and Gypsum are shown in Figures S5 and S6, respectively. On both materials, networks built using relative abundances were both sparser and less connected than with abundances adjusted using quantitative profiling.

4 | DISCUSSION

The application of multiple culture-independent quantitative microscopy techniques, both independently and in combination with 16S rRNA and ITS amplicon sequencing (quantitative profiling), provided deeper insight into the effects of water and high humidity on building material microbial growth. As we hypothesized, the quantitative data revealed strong differences between material types in both total bacterial and fungal loads and growth patterns over the course of the experiment (Figure 3). The combination of abundance data and sequence counts (ie, quantitative profiling) also clearly identified periods of both growth and decline of bacterial and fungal taxonomic groups not observable via relative abundance data (Figures 5 and 6). Moreover, quantitative profiling often directly contradicted conclusions based solely on relative abundance information for the same samples. Overall, our results strongly suggested that combining quantitative and qualitative data not only improves the understanding of BE microbiome dynamics but also avoids incorrect inferences made from analyses based on relative abundances, particularly in high growth conditions.

Microscopy analysis also provided unexpected insight into material- and time-dependent difference in fungal growth morphology. Close examination of the gypsum fungal growth patterns showed a significant change in growth morphology from spores to hyphae starting at week three. By T5, hyphae dominated the gypsum coupons (Figure 3B; Figure 4). Many fungal species are known to be "dimorphic" and have the ability to switch between a unicellular yeast-like form and a multicellular filamentous form in response to changing environmental conditions (temperature, pH and water availability) and/or cell densities (via quorum sensing).[57] Many fungi can reproduce in both form unicellular and multicellular forms, and some can do so reversibly. The "spores" we observed under the

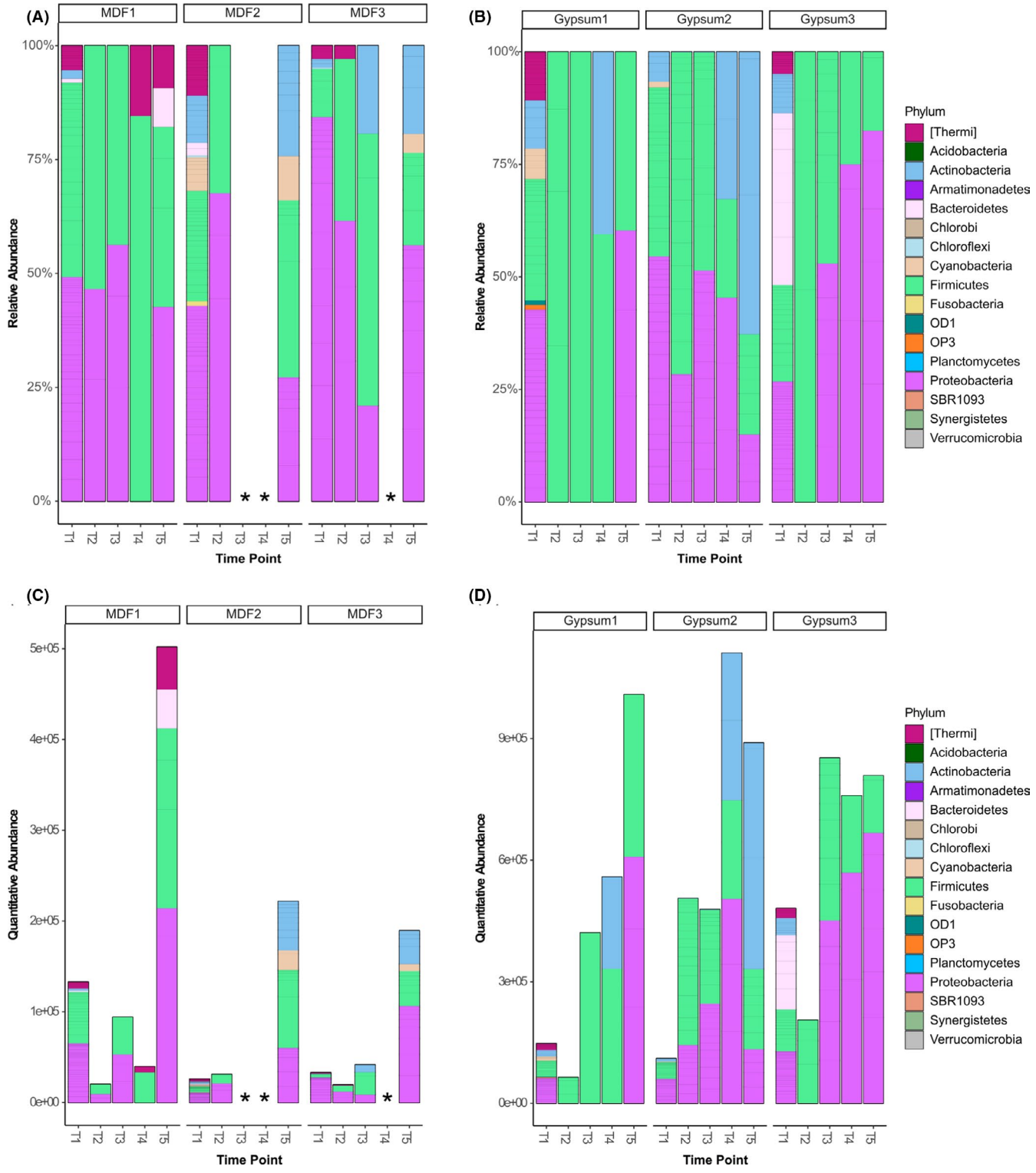

FIGURE 5 Bacteria taxonomy abundance for 16S rRNA whole samples on gypsum and MDF, comparing relative abundance (A, B) and quantitative abundance (C, D). Samples were grouped according to material type and coupon number, plotted from TP1 to TP5. (Note the different scales of the y-axis between (C) and (D).) The abundances of SVs that share the same Phylum classification were added together and shown in one color. All SVs in one sample were stacked. Samples with asterisks indicate no reads remained after DADA2 and classification filtering

microscope were likely the unicellular growth forms, and as the conditions changed over time on the gypsum, perhaps as a result of lower local water availability or cell densities, fungi switched from unicellular to multicellular growth by T3. With the MDF coupons, on the other hand, we suspect the environmental conditions or cell densities did not favor a switch in growth forms, which would explain

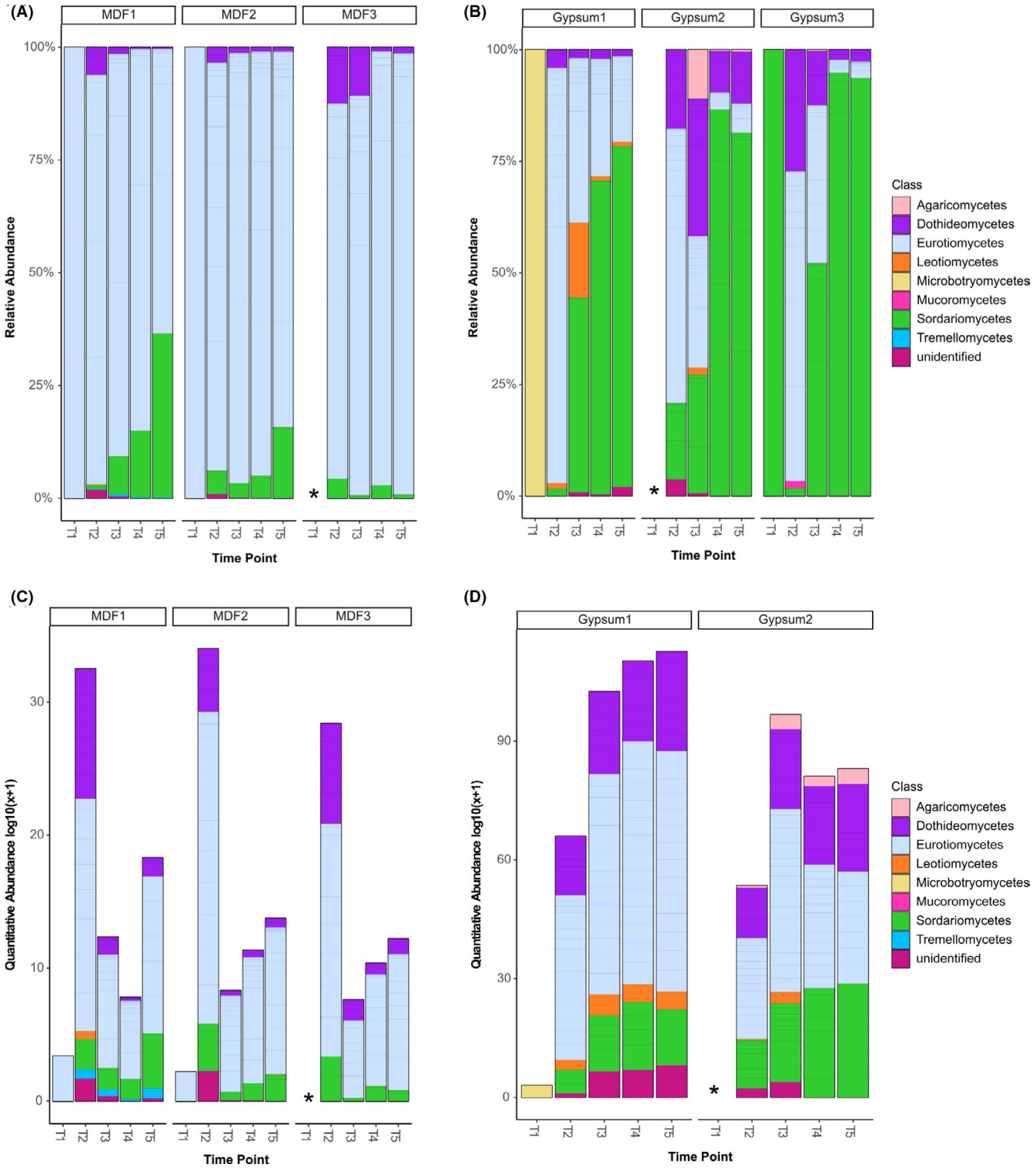

FIGURE 6 Fungi taxonomy abundance on gypsum and MDF, comparing relative abundance (A, B) and quantitative abundance (C, D). The log10 transformed abundances of SVs that share the same Class classification were added together and showed in one color. (Note the different scales of the y-axis between (C) and (D)). Quantitative abundance was not applied to gypsum3 coupon since fungi spore counts and hyphae length were not calculated for that coupon

the lack of observed hyphal growth. Our personal observations indicated that the MDF coupons became much drier after T2 while the gypsum coupons remained wet throughout. Future work should include measurements of moisture content of specific material to determine how locally available water and material porosity affects growth patterns and fungal dimorphism.

As with previous studies,[20,21] we determined a strong positive correlation between bacteria and VLPs (r = 0.81; Table 1) but also

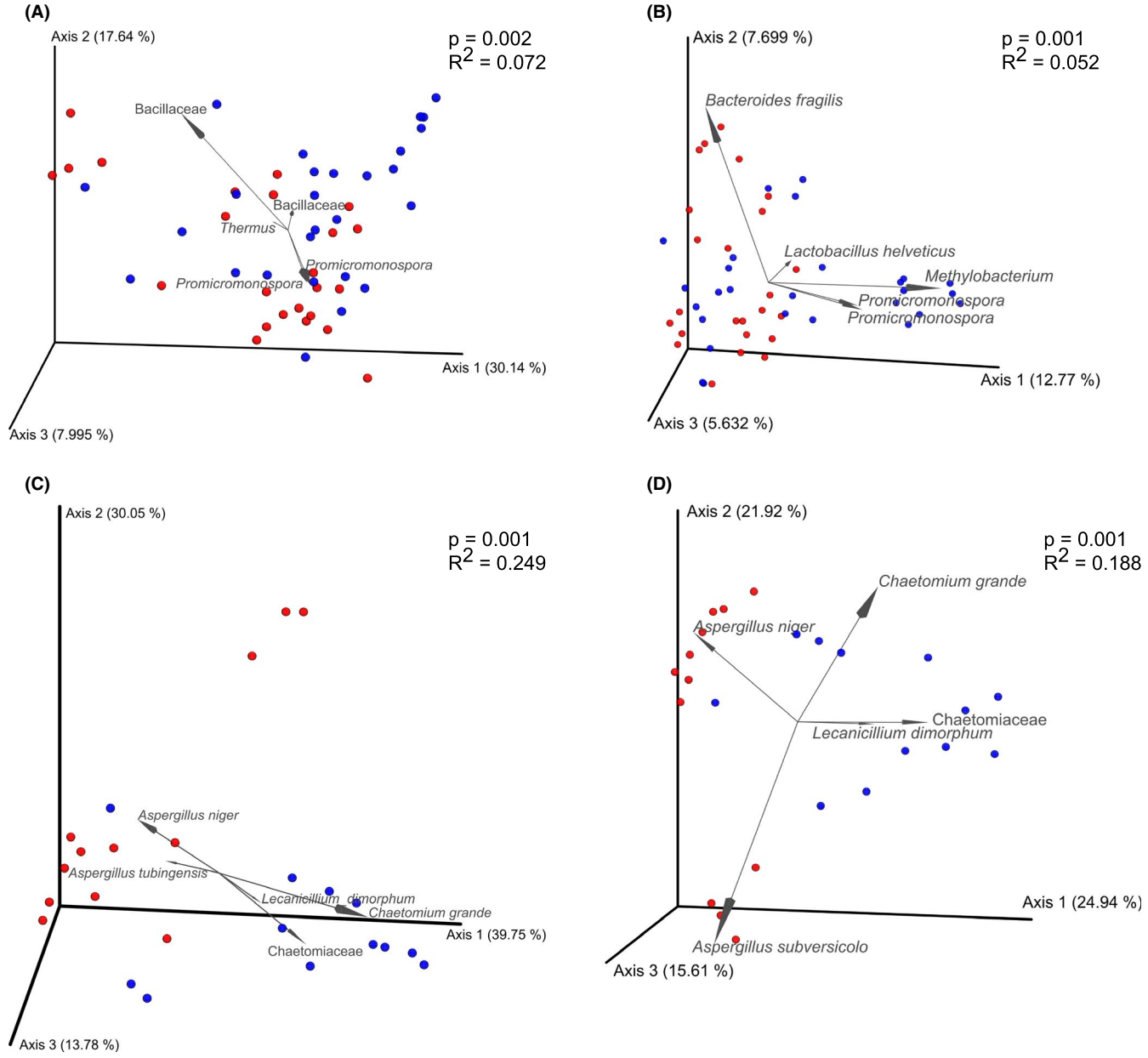

FIGURE 7 PCoA biplot in three-dimensional space. 16S rRNA samples represented using weighted UniFrac distances (A) and Bray-Curtis distances (B). ITS samples represented using weighted UniFrac distances (C) and Bray-Curtis distances (D). Gypsum samples are shown in blue while MDF samples are shown in red. Feature tables were rarefied to even sampling depth and converted to relative abundances. The three axes indicate the top three principle components with numbers in parenthesis explaining sample variation. Vectors all start from center (0,0,0), labeled in the lowest classified taxonomy level. Smaller angle between two vectors represents higher positive correlation, while two vectors pointing to opposite directions show a high negative correlation

a positive correlation between bacterial and fungal spore counts (r = 0.5; Table 1). The strong bacteria-VLP correlation was likely because the VLP were mainly bacteriophage. The bacteria-fungi correlation, on the other hand, may have indicated that the growth conditions (water, high humidity) and substrate availability generally favored microbial growth, especially on gypsum. It is also possible that some synergy existed between fungi and bacteria. However, unlike with gypsum, bacterial and fungal growth patterns diverged on MDF coupons and there was a significant interaction between fungal spore counts and material type (Table 2).

Direct microscopic examination of fungal diversity identified *Ulocladium*, *Alternaria* and *Chaetomium* spores based on their physical appearance and characteristics (Figure S3). These genera are commonly associated with water-damaged and damp buildings.[58,59] Many indoor fungi, including *Chaetomium*, secrete enzymes to breakdown cellulose and lignin in paper and wood to produce easily assimilated molecules.[60] These cellulose-derived products can also fuel subsequent microbial growth. Spores from *Alternaria* species have been identified on water-damaged surfaces and are known allergens that have been identified as a risk

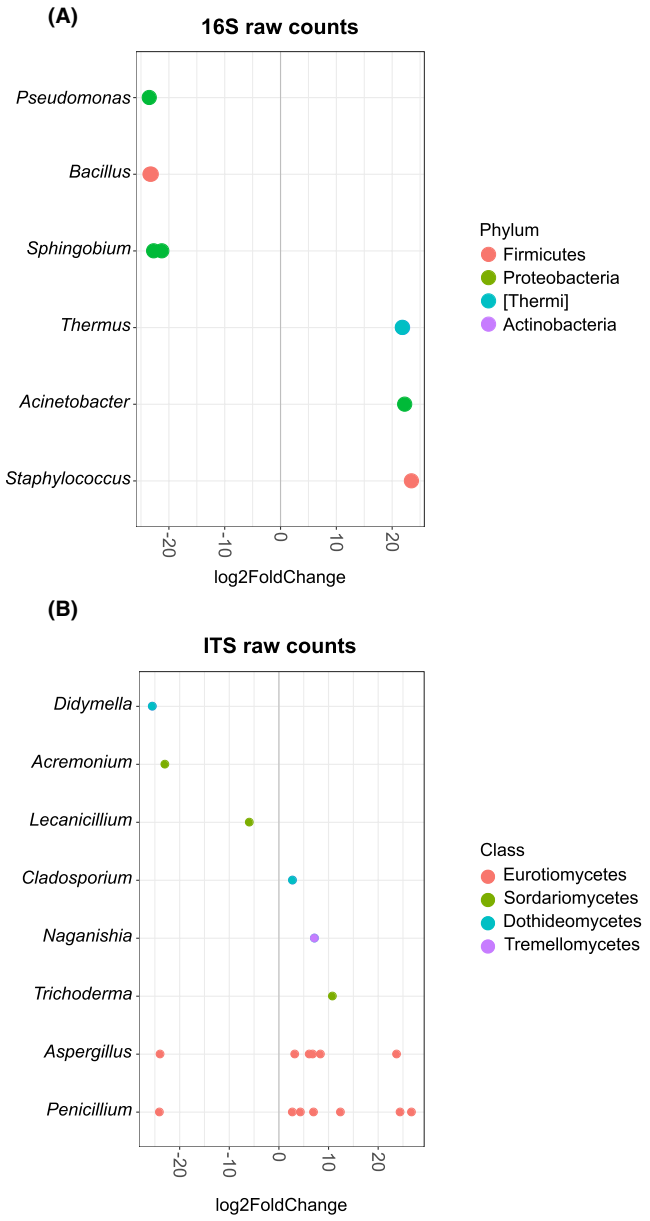

FIGURE 8 Log_2-fold analysis for taxonomic abundance differentiation on MDF relative to gypsum (MDF/gypsum) comparing 16S rRNA whole samples (A) and ITS samples with raw counts (B). Each dot represents a SV, and those share the same genus classification are shown on the same line. SVs are also colored according to its classification in class level for comparison at a higher level. Positive log_2 values indicate the organism being more abundant on MDF surfaces relative to gypsum surfaces, vice versa

factor for the development and persistence of asthma.[61,62] Both *Ulocladium* and *Chaetomium* are cellulolytic fungi and tertiary colonizers, and the presence of these fungi has been used as an indicator of long-term water damage.[60]

Overall, our microbial biomass analysis of the wetted BE materials provided at least as strong a signal of the effects of material type and time as did sequence-based taxonomic profiling. Not only was the overall bacterial and fungal biomass higher on gypsum than MDF coupons, but we also observed differential time-dependent growth patterns on the two materials (Table 2; Figure S2), and highly differentiated fungal growth morphologies (Figure 3B). FACS analysis of live and dead bacterial cells also identified differences between the material types. FACS confirmed there were substantial numbers of live cells on both materials types, and by week 2, gypsum coupons had higher ratios of live to dead cells than MDF coupons. On MDF coupons, the proportion of live cells did not exceed the number of dead cells until the third week of the experiment (Figure S4) and there was a significant interaction between material type and the live cell FACS counts (Table 3).

4.1 | Bacterial and fungal community dynamics

Incorporation of quantitative bacterial count and fungal biomass information made a dramatic difference in the interpretation of bacterial and fungal community growth dynamics. At the phylum level, the quantitative microbial profiling results often contradicted the relative profile interpretations. For example, relative profiling indicated a negative abundance relationship between the Firmicutes and the Proteobacteria (Figure 5A). However, quantitative profile shows this pattern was clearly an artifact. For example, the relative increase in Firmicutes from T3 to T4 on MDF1 was entirely a result of a decrease in Proteobacteria, while Firmicute abundance remained unchanged (Figure 5C). In other cases, when the relative abundance indicated a decrease in a particular taxonomic group from one time point to the next, quantitative profiling showed an *increase* in this phylum's abundance. For example, from T3 to T4 on coupon Gypsum2 we observed a decrease in the relative abundance of Proteobacteria (Figure 5B), but in fact Proteobacteria actually increased in number, a pattern obscured by the greater increase in the number of Actinobacteria (Figure 5D).

Similar patterns were observed in the comparisons of fungal relative and quantitative profiling. For instance, the relative abundances of Sordariomycetes and Eurotiomycetes appeared mutually exclusive in the relative abundance profiling (Figure 6A, B). However, these negative correlations appeared to be an artifact of the compositional nature of the data. For example, on coupon MDF2 the relative abundance of Eurotiomycetes decreased from T1 to T2 (Figure 6A), but the quantitative profiling indicated a large *increase* of Eurotiomycetes, a pattern undetectable via relative profiling because of the relative increase of Sordariomycetes and Dothideomycetes (Figure 6C). Similar patterns can be observed with gypsum (eg, T1 to T2 on Gypsum1; Figure 6D). As with the bacteria, we also observed many instances in which a small change in relative profiling actually corresponded to a large change in quantitative abundance (eg, T2 to T3 on MDF2; Figure 9C). These results showed not only the power and clarity of quantitative profiling for describing microbial communities, but also the usefulness of longitudinal analyses and repeated measures for determining whether changes in microbial diversity are the results of growth or decline of particular organisms.

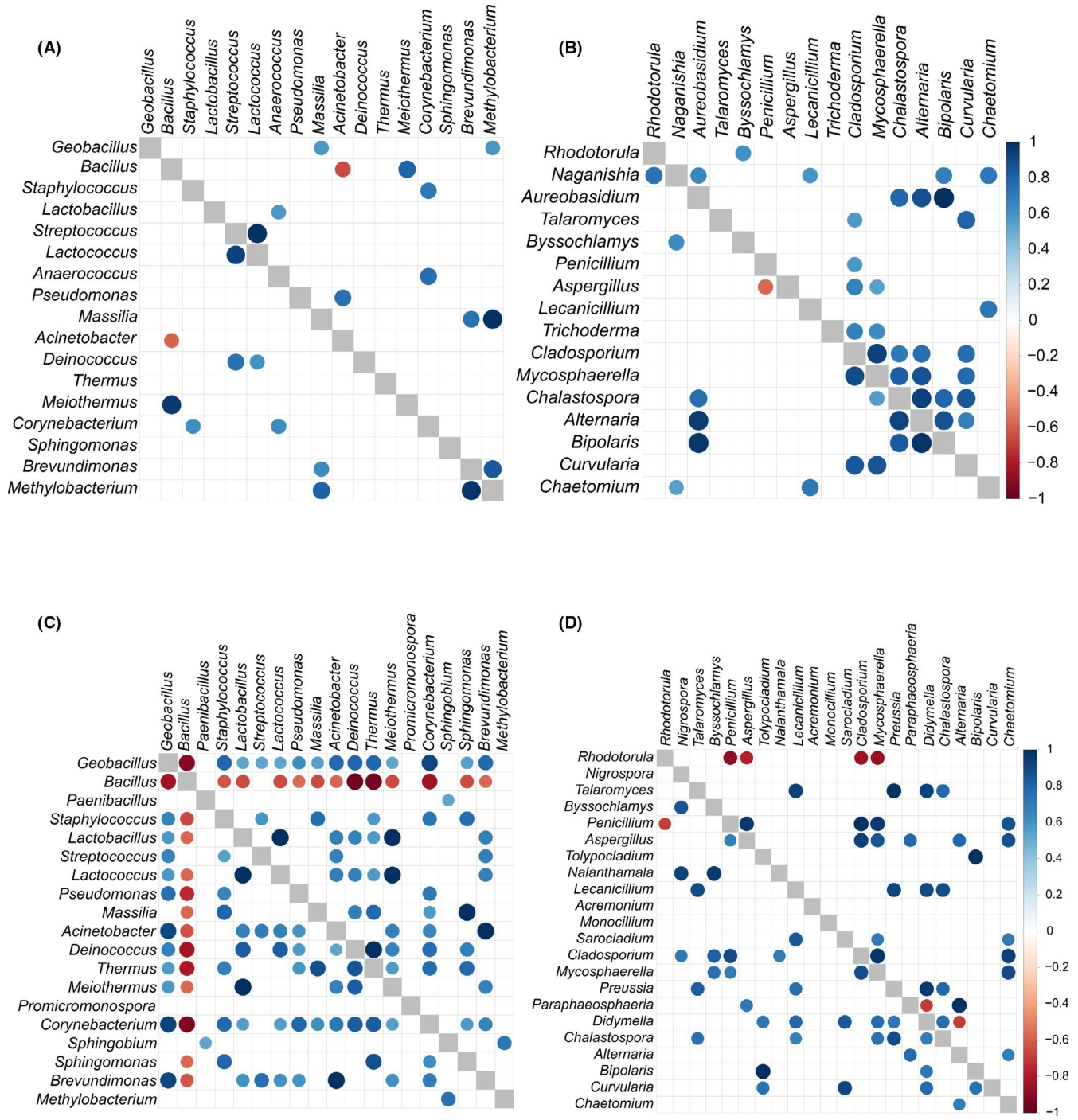

FIGURE 9 Correlation matrix for bacteria (A) and fungi (B) on MDF surfaces and bacteria (C) and fungi (D) on gypsum surfaces. The dots represent r values: only significant correlations with $r > 0.3$ (Pearson's r) and $P < .05$ are shown. Red dots represent negative correlations, and blue dots represent positive correlations. Lower triangle shows r values calculated with relative abundance, while upper triangle shows r values calculated with quantitative abundance

Analysis of community beta-diversity indicated strong associations between material type and both bacterial and fungal community composition (Figure 7). PCoA biplot analysis found several bacterial genera strongly associated with gypsum, namely, *Bacillus*, *Methylobacterium*, and *Promicromonospora* (Figure 7A,B). These three genera are common in the BE and *Methylobacterium* occur in high abundance in moist environments (eg, leaf surfaces) and are highly abundant in wet BE environments, such as shower curtains, tap water, and sinks.[4,63] There also has been study showing *Promicromonospora* was isolated from indoor wall material under moisture condition.[64] The log2fold change analysis also several bacterial genera highly differentiated between

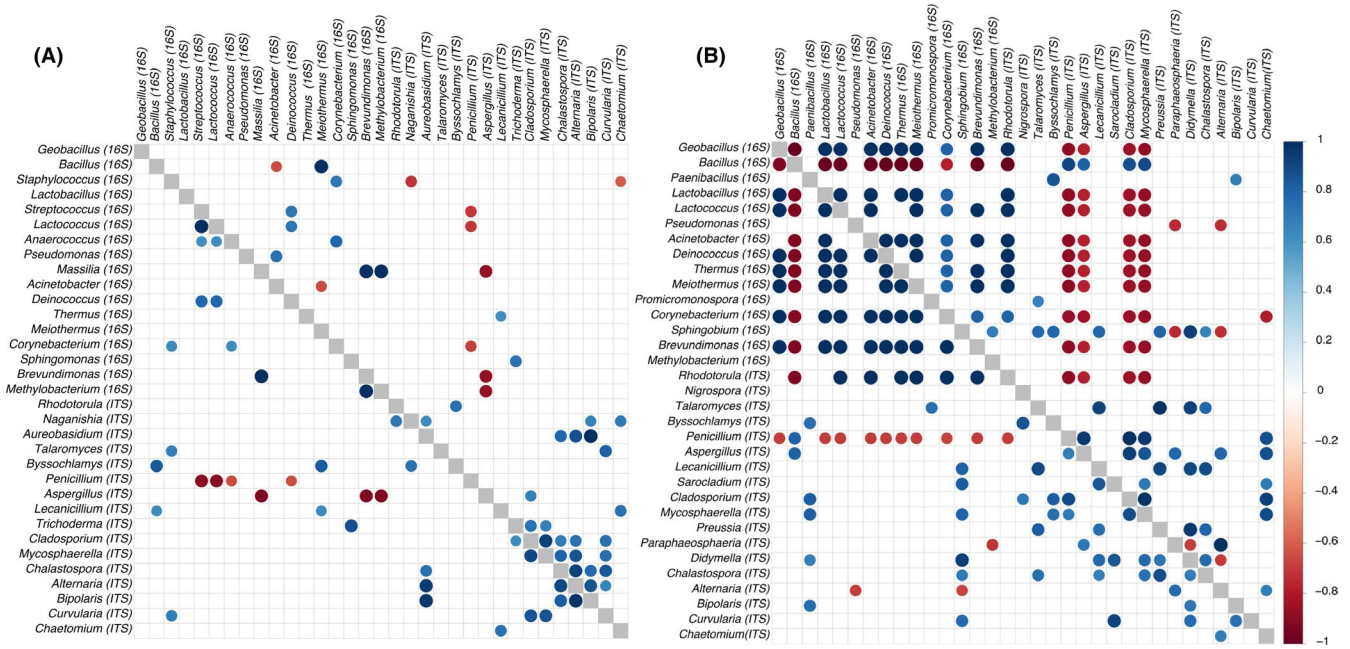

FIGURE 10 Correlation matrix for bacteria and fungi community combined on MDF (A) and gypsum (B) surfaces. The correlation analysis only included samples that had sequence libraries for both 16S and ITS, and both bacterial cell counts and fungal biomass microscopic quantitation. The dots represent r values: only significant correlations with $r > 0.3$ (Pearson's r) and $P < .05$ are shown. Red dots represent negative correlations, and blue dots represent positive correlations. Lower triangle shows r values calculated with relative abundance, while upper triangle shows r values calculated with quantitative abundance

MDF and gypsum. Gypsum harbored a higher proportion of wet-adapted species relative to MDF common in indoor settings such as *Pseudomonas*, *Bacillus*, and *Sphingobium*, whereas MDF had higher relative numbers of desiccation tolerant genera such as *Thermus* and *Staphylococcus* (Figure 8A). In the fungal community, the weighted UniFrac distance-based analysis also showed that gypsum samples were positively correlated with axis1 along with *Chaetomiaceae* and *Lecanicillium* (Figure 7C). Both of these fungal genera belong to Sordariomycete class of fungi which is known to be plant and animal pathogens and mycoparasites.[65] Both are also known to grow well on rotting woods, and cellulose has long been known to be a rich growth substrate for *Chaetomiaceae*.[66] *Aspergillus*, a member of the Trichocomaceae family, was negatively correlated with axis1 and therefore associated with MDF. Trichocomaceae tend to be associated with food spoilage and mycotoxin production. They can occur in indoor environments and cause health hazards by releasing mycotoxins and surface proteins.[67]

Introducing quantitative data into correlation and network analyses changed the overall number of correlations on both MDF and gypsum (Figure 9), but particularly with the fungi-fungi correlations on MDF (Figure 9B). We also noticed a general increase in the overall connectivity of the correlation networks on both MDF and gypsum (Figures S5 and S6). While the majority of the correlations identified with relative abundance data were also present with the quantitative data, some were no longer detected, such as the negative correlations between *Aspergillus* and *Penicillium* on MDF (Figure 9B). On the other hand, on gypsum we determined some novel negative correlations between *Rhodoturla* and *Aspergillus*, *Cladosporium and Mycosphaerella*; *Paraphaeosphaeria* and *Didymella*; and *Didymella* and *Alternaria* (Figure 9D). Species of *Rhodoturla* are common indoor yeast-like fungi that have emerged over the last two decades as serious opportunistic pathogens for immunocompromised and hospitalized patients.[68] Identifying organisms with negative abundance patterns could potentially be used to identify antifungal molecules for controlling *Rhodoturla* infections. Moreover, our study helped identify the types of building materials (eg, gypsum) and conditions are most likely to encourage the growth of *Rhodoturla* and other possible pathogenic microbes.

One set of correlations detected in both relative and quantitative correlation tables, was the negative correlation between *Bacillus* and 12 different bacterial genera on gypsum, especially *Geobacillus* (Figure 9C). Interestingly, the correlation matrix of bacteria and fungi on Gypsum also showed that *Penicillium* was negatively correlated with all the same bacteria as *Bacillus*, but positive correlated with *Bacillus* (Figure 10). In fact, the addition of quantitative data indicated that four different fungal genera, *Penicillium*, *Aspergillus*, *Cladosporium*, and *Mycosphaerella*, were all negatively correlated with the same 10 bacterial genera, but also all positively correlated with *Bacillus* (Figure 10B). We suggest that *Penicillium* and these other fungi repressed the growth of these bacterial genera with antibiotics (ie, penicillin), a situation which favors the growth of the *Bacillus*, a soil organisms that interacts in nature with these fungi and which is known to be antibiotic-resistant.[69] To test this hypothesis, future work could involve direct co-culturing of

BE *Penicillium* isolates with BE isolated bacteria, such as strains of *Bacillus* and *Geobacillus*.

5 | CONCLUSION

Overall, our results show the power of introducing quantitative biomass measures into BE microbial community analyses, particularly in actively growing environments. These data were particularly enlightening when combined with a longitudinal study design. With this combination, we were able to show that both biomass and growth patterns differed markedly on materials and over time and that incorporation of quantitative data in taxonomic profiling can significantly alter interpretations of microbial diversity. In particular, the incorporation of quantitative information highlighted differences in microbial community growth on the two materials, MDF and gypsum. While differences in chemical composition between MDF and gypsum probably played a role in selecting for such radically different community dynamics, physical differences may have also contributed. The gypsum paper was thinner than the MDF material and appeared to remain moister throughout the experiment, likely encouraging more microbial growth. Future quantitative studies should directly investigate the influence of water, chemistry, and porosity on microbial community composition. Our results also showed the importance of incorporating analysis of fungal community and abundance in addition to just looking at bacteria community especially when studying microorganism interactions and dynamics. A solitary focus on bacteria-bacteria interactions would have missed the fungi as being potential regulators of overall community dynamics.

ACKNOWLEDGEMENTS

We thank Stephen Head and the members of the TSRI Core Facility for help and advice with the sequencing. Cameron Smurthwaite is gratefully acknowledged for his input and assistance with the FACS analyses. This research was partially funded by a grant from the Alfred P. Sloan Foundation's Microbiology of the Built Environment Program: "Modeling Mechanisms of Microbial Succession in the Built Environment."

CONFLICT OF INTEREST

The authors have no conflicts of interest to declare.

AUTHOR CONTRIBUTION

Ying Xu: Conceptualization (supporting); Data curation (lead); Formal analysis (lead); Investigation (equal); Methodology (equal); Software (lead); Validation (equal); Writing-original draft (equal); Writing-review & editing (equal). **Ruby Tandon:** Conceptualization (equal); Formal analysis (equal); Investigation (equal); Methodology (lead); Validation (equal); Visualization (supporting); Writing-original draft (equal). **Chrislyn Ancheta:** Investigation (supporting); Methodology (supporting); Visualization (supporting). **Pablo Arroyo:** Investigation (supporting); Methodology (supporting). **Jack A. Gilbert:** Funding acquisition (equal); Methodology (supporting); Writing-review & editing (supporting). **Brent Stephens:** Conceptualization (supporting); Methodology (supporting); Writing-review & editing (supporting). **Scott T. Kelley:** Conceptualization (lead); Funding acquisition (equal); Investigation (equal); Methodology (equal); Project administration (lead); Resources (lead); Software (supporting); Supervision (lead); Validation (equal); Visualization (supporting); Writing-original draft (supporting); Writing-review & editing (lead).

PEER REVIEW

The peer review history for this article is available at https://publons.com/publon/10.1111/ina.12727.

DATA AVAILABILITY STATEMENT

The data that support the findings of this study are openly available in European Nucleotide Archive at https://www.ebi.ac.uk/ena/browser/home, reference number PRJEB36066.

ORCID

Brent Stephens https://orcid.org/0000-0002-0177-6703
Scott T. Kelley https://orcid.org/0000-0001-9547-4169

REFERENCES

1. Hoppe P, Martinac I. Indoor climate and air quality. Review of current and future topics in the field of ISB study group 10. *Int J Biometeorol*. 1998;42(1):1-7.
2. Kelley ST, Gilbert JA. Studying the microbiology of the indoor environment. *Genome Biol*. 2013;14(2):202.
3. Gilbert JA, Stephens B. Microbiology of the built environment. *Nat Rev Microbiol*. 2018;16(11):661–670.
4. Kelley ST, Theisen U, Angenent LT, St. Amand A, Pace NR. Molecular analysis of shower curtain biofilm microbes. *Appl Environ Microbiol*. 2004;70(7):4187-4192.
5. Kembel SW, Jones E, Kline J, et al. Architectural design influences the diversity and structure of the built environment microbiome. *ISME J*. 2012;6(8):1469-1479.
6. Rintala H, Pitkaranta M, Toivola M, Paulin L, Nevalainen A. Diversity and seasonal dynamics of bacterial community in indoor environment. *BMC Microbiol*. 2008;8(1):56.
7. Tringe SG, Zhang T, Liu X, et al. The Airborne Metagenome in an indoor urban environment. *PLoS ONE*. 2008;3(4):e1862.
8. Yooseph S, Andrews-Pfannkoch C, Tenney A, et al. A metagenomic framework for the study of airborne microbial communities. *PLoS One*. 2013;8(12):e81862.
9. Gibbons SM. The built environment Is a microbial wasteland. *mSystems*. 2016;1(2):e00033-16.
10. Adams RI, Lymperopoulou DS, Misztal PK, et al. Microbes and associated soluble and volatile chemicals on periodically wet household surfaces. *Microbiome*. 2017;5(1):128–143.
11. Mensah-Attipoe J, Reponen T, Salmela A, Veijalainen AM, Pasanen P. Susceptibility of green and conventional building materials to microbial growth. *Indoor Air*. 2015;25(3):273-284.
12. Coombs K, Vesper S, Green BJ, Yermakov M, Reponen T. Fungal microbiomes associated with green and non-green building materials. *Int Biodeterior Biodegrad*. 2017;125:251-257.
13. Stephens B. What have we learned about the microbiomes of indoor environments? *mSystems*. 2016;1(4):e00083-16.
14. Chase J, Fouquier J, Zare M, et al. Geography and location are the primary drivers of office microbiome composition. *mSystems*. 2016;1(2):e00022-16.

15. Pasanen AL, Kasanen JP, Rautiala S, et al. Fungal growth and survival in building materials under fluctuating moisture and temperature conditions. *Int Biodeterior Biodegrad*. 2000;46(2):117-127.
16. Johansson P, Ekstrand-Tobin A, Svensson T, Bok G. Laboratory study to determine the critical moisture level for mould growth on building materials. *Int Biodeterior Biodegrad*. 2012;73:23-32.
17. Hoang CP, Kinney KA, Corsi RL, Szaniszlo PJ. Resistance of green building materials to fungal growth. *Int Biodeterior Biodegrad*. 2010;64(2):104-113.
18. Dedesko S, Siegel JA. Moisture parameters and fungal communities associated with gypsum drywall in buildings. *Microbiome*. 2015;3(1):71.
19. LBNL. Prevalence of building dampness; 2009. https://iaqscience.lbl.gov/dampness-prevalence. Accessed October 26, 2018.
20. LBNL. Nature and causes of building dampness; 2009. https://iaqscience.lbl.gov/dampness-nature. Accessed October 26, 2018.
21. Roze L, Hong S, Linz J. Aflatoxin biosynthesis: current frontiers. *Annu Rev Food Sci Technol*. 2013;4:293-311.
22. Miller JD, McMullin DR. Fungal secondary metabolites as harmful indoor air contaminants: 10 years on. *Appl Microbiol Biotechnol*. 2014;98(24):9953–9966.
23. Mendell MJ, Mirer AG, Cheung K, Tong M, Douwes J. Respiratory and allergic health effects of dampness, mold, and dampness-related agents: A review of the epidemiologic evidence. *Environ Health Perspect*. 2011;119(6):748-756.
24. Quansah R, Jaakkola MS, Hugg TT, Heikkinen SAM, Jaakkola JJK. Residential dampness and molds and the risk of developing asthma: A Systematic Review and Meta-Analysis. *PLoS One*. 2012;7(11):e47526.
25. Fisk WJ, Eliseeva EA, Mendell MJ. Association of residential dampness and mold with respiratory tract infections and bronchitis: A meta-analysis. *Environ Heal A Glob Access Sci Source*. 2010;9(1):72.
26. Lax S, Cardona C, Zhao D, et al. Microbial and metabolic succession on common building materials under high humidity conditions. *Nat Commun*. 2019;10(1):1767.
27. Sano E, Carlson S, Wegley L, Rohwer F. Movement of viruses between biomes. *Appl Environ Microbiol*. 2004;70(10):5842-5846.
28. McDaniel L, Breitbart M, Mobberley J, et al. Metagenomic analysis of lysogeny in Tampa Bay: Implications for prophage gene expression. *PLoS One*. 2008;3(9):e3263.
29. Bayer K, Kamke J, Hentschel U. Quantification of bacterial and archaeal symbionts in high and low microbial abundance sponges using real-time PCR. *FEMS Microbiol Ecol*. 2014;89(3):679–690.
30. Davis C. Enumeration of probiotic strains: Review of culture-dependent and alternative techniques to quantify viable bacteria. *J Microbiol Methods*. 2014;103:9-17.
31. Gibbons SM, Schwartz T, Fouquier J, et al. Ecological succession and viability of human-associated microbiota on restroom surfaces. *Appl Environ Microbiol*. 2015;81(2):765-773.
32. Prussin AJ, Garcia EB, Marr LC. Total concentrations of virus and bacteria in indoor and outdoor air. *Environ Sci Technol Lett*. 2015;2(4):84-88.
33. Greenspan L. Humidity fixed points of binary saturated aqueous solutions. *J Res Natl Bur Stand Sect A Phys Chem*. 1977;81A(1):89.
34. Schneider CA, Rasband WS, Eliceiri KW. NIH Image to ImageJ: 25 years of image analysis. *Nat Methods*. 2012;9(7):671-675.
35. Walters W, Hyde ER, Berg-Lyons D, et al. Improved bacterial 16S rRNA Gene (V4 and V4–5) and fungal internal transcribed spacer marker gene primers for microbial community surveys. *mSystems*. 2016;1(1):4-5.
36. Caporaso JG, Kuczynski J, Stombaugh J, et al. QIIME allows analysis of high-throughput community sequencing data. *Nat Methods*. 2010;7(5):335-336.
37. Bolyen E, Dillon M, Bokulich N, et al. Reproducible, interactive, scalable, and extensible microbiome data science using QIIME 2. *Nat Comm*. 2019;37(8):852–857.
38. Callahan BJ, McMurdie PJ, Rosen MJ, Han AW, Johnson AJA, Holmes SP. DADA2: High-resolution sample inference from Illumina amplicon data. *Nat Methods*. 2016;13(7):581-583.
39. Bokulich NA, Kaehler BD, Rideout JR, et al. Optimizing taxonomic classification of marker-gene amplicon sequences with QIIME 2's q2-feature-classifier plugin. *Microbiome*. 2018;6(1):90.
40. Katoh K, Standley DM. MAFFT multiple sequence alignment software version 7: Improvements in performance and usability. *Mol Biol Evol*. 2013;30(4):772-780.
41. Price MN, Dehal PS, Arkin AP. FastTree 2 - Approximately maximum-likelihood trees for large alignments. *PLoS One*. 2010;5(3):e9490.
42. Fouquier J, Rideout JR, Bolyen E, et al. Ghost-tree: Creating hybrid-gene phylogenetic trees for diversity analyses. *Microbiome*. 2016;4(1):11.
43. McDonald D, Clemente JC, Kuczynski J, et al. The Biological Observation Matrix (BIOM) format or: How I learned to stop worrying and love the ome-ome. *Gigascience*. 2012;1(1):7.
44. McMurdie PJ, Paulson JN. biomformat: An interface package for the BIOM file format; 2019. https://github.com/joey711/biomformat/, http://biom-format.org/. Accessed October 20, 2019.
45. R Core Team. *A language and environment for statistical computing*. Vienna, Austria: R Foundation for Statistical Computing; 2018.
46. McMurdie PJ, Holmes S. Phyloseq: An R Package for Reproducible Interactive Analysis and Graphics of Microbiome Census Data. *PLoS ONE*. 2013;8(4):e61217.
47. Hadley W. *Ggplot2: Elegant Graphics for Data Analysis*. New York, NY: Springer-Verlag; 2016.
48. Love MI, Huber W, Anders S. Moderated estimation of fold change and dispersion for RNA-seq data with DESeq2. *Genome Biol*. 2014;15(12):550.
49. Wei T, Simko V.R package "corrplot": Visualization of a correlation matrix. R Packag v 084; 2017.
50. Csardi G, Nepusz T. The igraph software package for complex network research. *InterJournal Complex Syst*. 2006(1695):2006.
51. Bray JR, Curtis JT. An Ordination of the upland forest communities of southern Wisconsin. *Ecol Monogr*. 1957;27(4):325-349.
52. Lozupone C, Knight R. UniFrac: A new phylogenetic method for comparing microbial communities. *Appl Environ Microbiol*. 2005;71(12):8228-8235.
53. Weiss S, Xu ZZ, Peddada S, et al. Normalization and microbial differential abundance strategies depend upon data characteristics. *Microbiome*. 2017;5(1):27.
54. Legendre P, Legendre L. *Numerical Ecology*, 3rd edn. Amsterdam: Elsevier; 2012.
55. Vázquez-Baeza Y, Pirrung M, Gonzalez A, Knight R. EMPeror: A tool for visualizing high-throughput microbial community data. *Gigascience*. 2013;2(1):16.
56. Vázquez-Baeza Y, Gonzalez A, Smarr L, et al. Bringing the dynamic microbiome to life with animations. *Cell Host Microbe*. 2017;21(1):7-10.
57. Nadal M, García-Pedrajas MD, Gold SE. Dimorphism in fungal plant pathogens. *FEMS Microbiol Lett*. 2008;284(2):127-134.
58. Gravesen S, Nielsen PA, Iversen R, Nielsen KF. Microfungal contamination of damp buildings - Examples of risk constructions and risk materials. *Environ Health Perspect*. 1999;107(suppl 3):505-508.
59. Andersen B, Dosen I, Lewinska AM, Nielsen KF. Pre-contamination of new gypsum wallboard with potentially harmful fungal species. *Indoor Air*. 2017;27(1):6-12.
60. Yang CS, Heinsohn PA. *Sampling and Analysis of Indoor Microorganisms*. Hoboken, NJ: Wiley-Interscience; 2007.

61. Andersson M, Downs S, Mitakakis T, Leuppi J, Marks G. Natural exposure to *Alternaria* spores induces allergic rhinitis symptoms in sensitized children. *Pediatr Allergy Immunol*. 2003;14:100–105.
62. Bush RK, Prochnau JJ *Alternaria*-induced asthma. *J Allergy Clin Immunol*. 2004;113(2):227-234.
63. Lee L, Tin S, Kelley ST. Culture-independent analysis of bacterial diversity in a child-care facility. *BMC Microbiol*. 2007;7(1):27.
64. Martin K, Schäfer J, Kämpfer P *Promicromonospora umidemergens sp. nov*., isolated from moisture from indoor wall material. *Int J Syst Evol Microbiol*. 2010;60(3):537-541.
65. Zhang N, Castlebury LA, Miller AN, et al. An overview of the systematics of the Sordariomycetes based on a four-gene phylogeny. *Mycologia*. 2006;98(6):1076-1087.
66. Ames LM. *A Monograph of the Chaetomiaceae*. Washington, DC: US Army Research; 1961.
67. Houbraken J, Samson RA. Phylogeny of *Penicillium* and the segregation of Trichocomaceae into three families. *Stud Mycol*. 2011;70:1-51.
68. Gomez-Lopez A, Mellado E, Rodriguez-Tudela JL, Cuenca-Estrella M. Susceptibility profile of 29 clinical isolates of *Rhodotorula spp*. and literature review. *J Antimicrob Chemother*. 2005;55(3):312-316.
69. Fenselau C, Havey C, Teerakulkittipong N, Swatkoski S, Laine O, Edwards N. Identification of β-lactamase in antibiotic-resistant *Bacillus cereus* spores. *Appl Environ Microbiol*. 2008;74(3):904-906.
70. Vandeputte D, Kathagen G, D'Hoe K, et al. Quantitative microbiome profiling links gut community variation to microbial load. *Nature*. 2017;551(7681):507-511.

SUPPORTING INFORMATION

Additional supporting information may be found online in the Supporting Information section.

How to cite this article: Xu Y, Tandon R, Ancheta C, et al. Quantitative profiling of built environment bacterial and fungal communities reveals dynamic material dependent growth patterns and microbial interactions. *Indoor Air*. 2020;00:1–18. https://doi.org/10.1111/ina.12727